# Seismic characteristics and distribution of Neogene deep-water turbidites in East Coast Basin, Offshore Hawke Bay, New Zealand

Che-Azlan Chemong[1*] and Sukonmeth Jitmahantakul[1]

[1] M.Sc. Petroleum Geoscience Program, Department of Geology, Faculty of Science, Chulalongkorn University, Bangkok, 10330, Thailand

*Corresponding author e-mail: Che-AzlanC@pttep.com

*Received:* 21 Jun 2022
*Revised:* 19 Jul 2022
*Accepted:* 19 Jul 2022

## Abstract

This paper presents seismic characteristics and distribution of Neogene deep-water turbidites in the Offshore Hawke Bay, New Zealand using 3D seismic data and seismic attributes analysis. Four main seismic facies were defined (facies A-D) within the Pliocene-Miocene interval. Additional horizons were interpreted to highlight possible turbidite depositional area. In the Miocene interval, the turbidite system pathways can be separated into three zones. First zone is the path where sediments are transferred from the SW high to the NE direction. The second zone is the pathway from N high. The third zone is located on the SE high, which was a paleo low. A simplified model of possible turbidite fairways was proposed with suggestion on the prospective location of turbidite fairways.

**Keywords:** Seismic characters, Neogene deep-water turbidites, Turbidites, East Coast Basin

## Introduction

The East Coast Basin (ECB) covers onshore and offshore areas of the eastern margin of the North Island, New Zealand (Fig. 1). The basin sits on the active convergent boundary between the Australian and Pacific plates (Lewis and Pettinga., 1993). The ECB is attractive due to its petroleum potential, which is proven by the significant quantity of onshore hydrocarbon seepages (Erdi and Huuse., 2018). These hydrocarbon seepages indicate that petroleum generation has already formed within the basin. During the early period of petroleum exploration in the ECB, small amounts of oil were produced from oil pits and shallow wells located close to the oil seepages in the 1870s (Field et al., 1997; NZP&M., 2014).

In the middle of the 1980s, a new period of exploration in the ECB commenced: extensive seismic surveys throughout the entire ECB anddrilling campaign of exploration wells (Dobbie and Carter, 1990; Field et al., 1997). Forty wells have been drilled onshore since then, resulting in the discovery of gas shows and high-pressure dry gas that are not commercially feasible.

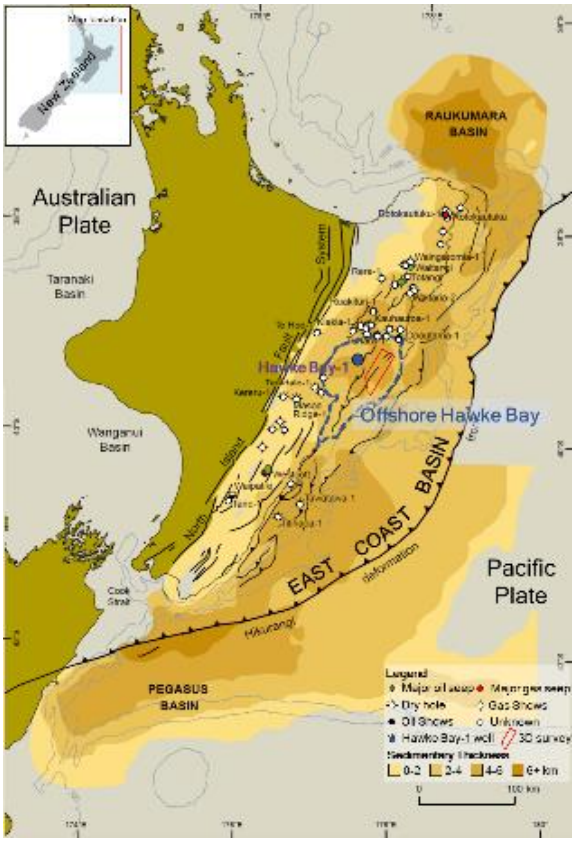


**Figure 1** Sedimentary thickness map of the East Coast Basin. Locations of the Offshore Hawke Bay (Navy blue polygon) and existing well are shown (modified after New Zealand Petroleum & Minerals, 2014).

In the offshore area, three exploration wells were drilled. The first offshore well (Hawke Bay-1) was drilled in 1976 by BP, Shell, Aquitaine, and Todd Energy (NZP&M., 2014). From the Hawke Bay-1 Well, only gas shows were found in the Oligocene limestone and the late Miocene turbidite sandstone was tight (NZP&M., 2014). The other two offshore wells (Tawatawa-1 and Titihaoa-1) had extensive gas shows in the Miocene intervals, however, they were not tested and were plugged and abandoned (NZP&M., 2014). Therefore, the offshore region of the ECB is still an underexplored area that has a high possibility of petroleum discovery.

According to previous studies in the ECB (Griffin et al., 2015; Darby et al., 2001 and Burgreen-Chan et al., 2015), the Cretaceous-Paleocene rocks are potential source rocks for petroleum, while the Eocene rocks are formed as a regional seal (Fig. 2). The primary reservoirs consist of Cretaceous shelfal and deep-water sandstones, Neogene shelfal and deep-water turbidite sandstones, and Neogene fractured limestones (Brown, 2002; Griffin et al., 2015). Hydrocarbon migration from source rocks can be inferred from seismic imaging of gas chimney above the Late Miocene normal faults (Erdi and Huuse, 2018).

This study focuses on the Neogene (Late Miocene) deep-water turbidites of the ECB. This stratigraphic unit has thickness of up to 6 kilometers and shows good reservoir properties (Erdi and Huuse., 2018). Several potential reservoir targets in Neogene, such as the Makareo Sandstone (28 percent porosity and 247 mD permeability) and the Tuhara Formation (20-23 percent porosity), had been reported (Brown., 2002). By conducting integrated geophysical analysis, the purpose of this study is to characterize the seismic facies of the Neogene deep-water turbidites in the offshore ECB in order to gain a better understanding of their occurrence, distribution, and reservoir potential for the purposes of petroleum exploration.

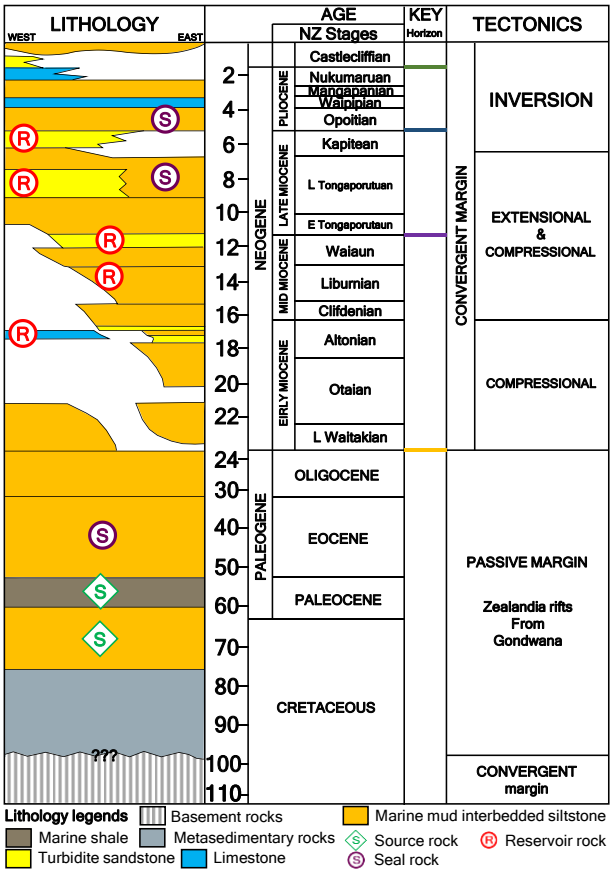


**Figure 2** General stratigraphy and key tectonic events of the ECB offshore Hawke Bay (modified after Brown, 2002)

## Geological Settings

The structural framework and sediment deposition in the ECB are controlled by three main tectonic events: Late Jurassic-Early Cretaceous convergent margin, Early Cretaceous-Oligocene passive margin, and Early Miocene-Recent convergent margin (Burgreen-Chan et al., 2015; Fig. 2).

The first compression was associated with the accretionary subduction complex along the Gondwana's margin during the Late Jurassic to Early Cetaceous (Mortimer., 2004; Burgreen-Chan et al., 2015). The metasedimentary rocks formed during this event becomes the basement rocks underneath the ECB.

In 100 Ma, the region was turned to passive margin settings. The Early Cretaceous turbiditic sediment was deposited and followed by the Late Cretaceous to Paleocene post-rift sequence (Burgreen-Chan, et al., 2015). These units consist of siliceous mudstone (Whangi Formation) and organic-rich mudstone (Waipama Formation) lying conformably. The Eocene to Oligocene sequences consist of smectite-rich and benthonic mudstone (Wanstead Formation) and calciferous massive mudstone (Weber Formation) (Brown., 2002; Burgreen-Chan., et al. 2015).

The second compression occurred in the Early Miocene. Approximately in 25 Ma, subduction along the Kermedec-Hikurangi trench reactivated the ECB to convergent margin (Burgreen-Chan et al. 2015). At bathyal depth, an Early Miocene mudstone sequence containing sandstone units rich in glauconite was deposited. This sequence was succeeded by Tunanui sandstones at deeper bathyal depth (Brown., 2002).

During the Middle-Late Miocene, gravity flow units of the Makaretu Formation were deposited on top of Tunanui sandstone and followed by mudstone-dominated units deposited at bathyal depth (Brown, 2002). The ECB was also affected by an extension causing the formation of normal faults in the basin (Erdi and Huuse., 2018).

In the Pliocene, regional compression resulted in inversion (Erdi and Huuse., 2018). The depositional environment was interpreted as outer shelf and slope settings, followed by shallow-marine shelf sediment package of Pleistocene-Holocene (Barnes et al., 2002; Paquet, et al., 2011).

Several Neogene deep-water turbidites have been investigated by onshore outcrop studies (e.g., Field et al., 2005; Francis., 1995). Deep-water, slope (channel and overbank), and basin-floor sandstones are the most widespread types of Neogene clastic reservoir lithologies expected in the offshore ECB (Francis et al., 2004; Field et al., 2005; Strogen et al., 2010; Griffin et al., 2015), since they were examined from analogous onshore outcrop units.

The Middle Miocene turbidite of the Tunanui Formation is also discovered at an outcrop locality in the forearc region near the town of Wairoa on New Zealand's northern island. It is composed of a thick succession of sand-rich mass-flow deposits and flow-stripped sandstones of ponded turbidites (Field et al., 2005). In addition, well information indicates thickness of approximately 265 m in Tuhara-1, 450 m in Mangaone-1, approximately 1000 m in Opoho-1, and 2700 m near Mangaone town (Field et al., 2005).

The Middle - Late Miocene Makaretu sandstone is considered as the primary reservoir target due to its broad regional unit (e.g., Francis., 1995, 1998; Davies et al., 2000; Mazengarb and Speden., 2000). In the northern region of Hawke's Bay, the outcrop exposes this unit in 230 meters thickness (Francis., 1995). Hawke Bay-1 drilled the lateral equivalence of this unit and encountered 95 meters in thickness. It was interpreted that the depositional environment was deep water turbidite fan with alternating sandstone-mudstone beds. Typically, sandstone comprises 90–95 percent of the rock's volume. The thickness of individual sandstone beds ranges from 0.5 to 15 meters (Francis., 1995). The Makaretu sandstone contains average helium porosity of 26.8% and air permeability of 203 mD (Francis., 1994).

## Datasets and methodology

This study used 3D seismic dataset acquired in 1999. The seismic data covers approximately 594 $km^2$ and the seismic cubes are oriented in NE-SW direction (Fig. 3). The data were processed to 6 s with bin size of 12.5 meters in both sides. The seismic quality is fair

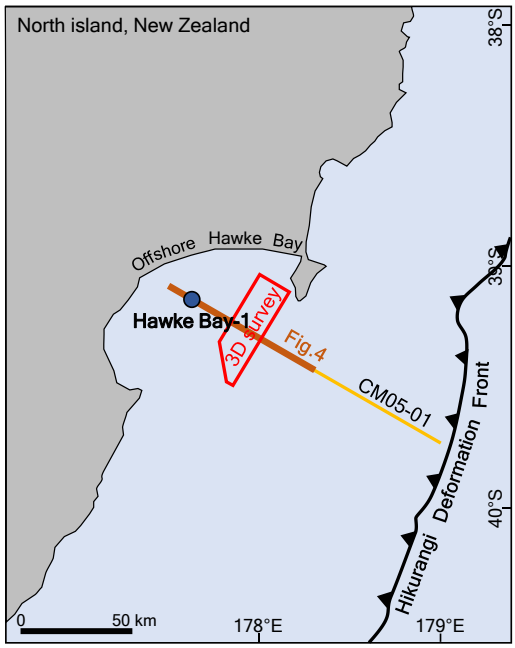


**Figure 3** Simplified map of the offshore Hawke Bay of the ECB showing locations of 2D and 3D seismic data, and Hawke Bay-1 well.

to good. The vertical seismic resolution ranges from 16 meters at the seabed to 89 meters at around 6 s (Erdi and Huuse, 2018).

The Hawke Bay-1 well is the only well available and it was used in this study. In order to pick key horizons from the well to the study area, 2D seismic line (05CM-01) was used for the regional interpretation and was tied to the 3D seismic data (Fig. 4).

This study interpreted the seismic stratigraphy with an emphasis on the Neogene packages by using Petrel 2017 and PaleoScan™ software. This study applied the PaleoScan™ software to build sub-horizons between the four main horizons by horizon stacking. The generation window included above Top Pliocene to below Top Oligocene. Over one hundred sub-horizons were generated. Following extracted seismic attribute as horizon attribute for turbidite architectural element identification. Seismic attributes, such as root mean square (RMS), sweetness, chaos, instantaneous frequency, and spectral decomposition, were produced along the sub-horizons which are the horizon stack output. These attribute maps can highlight some geological features that might be overlooked, including turbidite reservoirs.

## Results

### Seismic facies analysis

The analysis of 3D seismic data can provide a description of the seismic facies observed in the Neogene key sequences. The seismic reflector characteristics (amplitude, internal reflection, continuity, terminations, and architectural elements) allow to define main seismic facies that are associated with deep marine deposition. Table.1 contains a list of the seismic facies in the study area with the descriptions.

Seismic facies A is composed of discontinuous, high reflectors. The seismic facies are terminated by parallel reflectors of medium or low amplitude. Generally, the seismic facies are found on the foot-wall side of thrust fault and they might be related to structural control in the study area.

Seismic facies B is distinguished by its high, constant amplitude and flat, continuous reflector. This seismic facies may be associated with the channel in the lower part

The seismic facies C is characterized by continuous and low-to-moderate amplitude reflectors. Generally, the seismic reflectors are parallel to one another. In the Pliocene, they aggregate into very thick packages. Generally, they lie unconformably on deeper strata.

Seismic facies D is characterized by chaotic, discontinuous reflectors with moderately low amplitude. Typically, there is no internal reflection and the amplitude varies based on the contrast of the acoustic impedance (AI). The seismic facies consist of slump and slide deposits characteristics. This seismic facies is

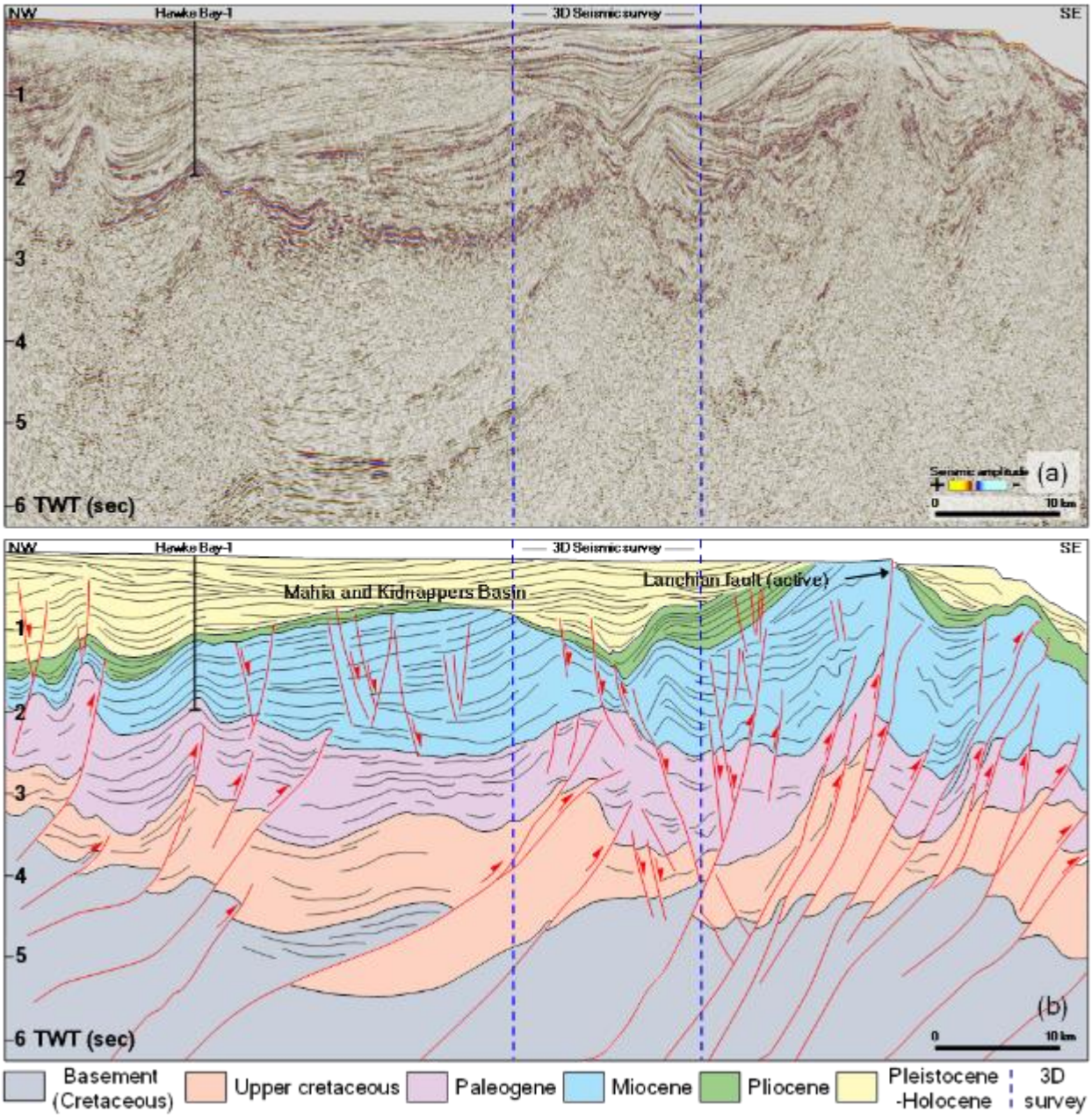


**Figure 4** (a) 05CM-01 2D seismic uninterpreted line (b) interpretation illustrating the regional structural framework of ECB and well constraining for seismic interpretation to 3D seismic survey. Line location is shown in Figure 3.

classified as a mass transportation deposit, flowing from the local high area in the east to the west direction.

## Seismic stratigraphy

In this study, detailed seismic stratigraphy of the Neogene succession was investigated and used in reservoir characterization. Following information from the Hawke Bay-1 well, the strata of the Paleogene sequence, Early-Middle Miocene sequence, Late Miocene sequence, and Pliocene sequence were correlated with seismic data. Five key seismic horizons (Top Pliocene, Top Late Miocene, Top Middle Miocene and Top Oligocene) were initially interpreted and

| Seismic Facies | Schematic | Seismic character |
|---|---|---|
| 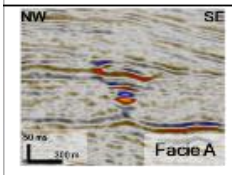  | 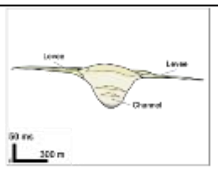 | High amplitude, Subparallel reflectors, terminated with parallel reflectors of medium or low amplitude |
| 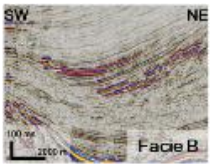  | 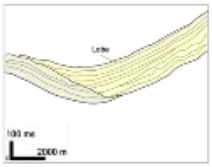 | High amplitude, Parallel to subparallel and good continuity reflectors |
| 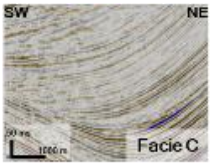  | 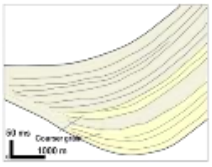 | Low to moderate amplitude, Parallel to subparallel reflectors and often low signal to noise ratio. |
| 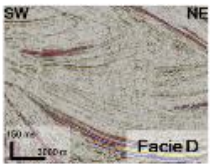  | 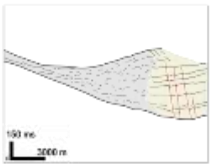 | Generally low amplitude (variable depends on acoustic impedance contrast), Subparallel to chaotic |

**Table 1** Seismic facies observed on 3D seismic data with the description of reflection characteristics.

mapped. Seismic sequences bounded by these horizons can be described as follows:

**Paleogene sequence**

The Hawke Bay-1 well reached the upper Paleocene section. Thus, the Top Oligocene was picked and correlated to the 3D seismic data. On the seismic data, the top of this sequence is characterized by moderate to high amplitude reflection. In the study area, the main seismic character is sub horizontal reflection and it is consistent with the Cretaceous sequence below.

**Early-Middle Miocene sequence**

The Early-Middle Miocene sequence is marked by the Top Middle Miocene horizon. This sequence is characterized by moderate to high positive amplitude reflection. The main seismic character is sub horizontal reflection, consistent with the Paleogene sequence below. In the southwest structural high of the study area, the top of this sequence was eroded and truncated by the Pliocene sequence (Fig.5b).

**Late Miocene sequence**

The Top Late Miocene seismic horizon marks the top of the Late Miocene sequence. This sequence is characterized by high positive amplitude reflection. In the southeastern part of the study area, early fill of this sequence shows growth strata in the seismic section (Fig.5b). The top of this sequence was eroded and truncated by the Pliocene sequence. It is related to structural high in the southeastern area (Fig.5b).

**Pliocene sequence**

The Pliocene sequence is characterized by high, positive amplitude reflection. The top of this sequence was eroded and truncated by the Holocene-Pleistocene sequence (Fig.5b). In the northwestern part of the study area, the seismic characteristics shows wedge-shaped geometry oriented to northeastern direction.

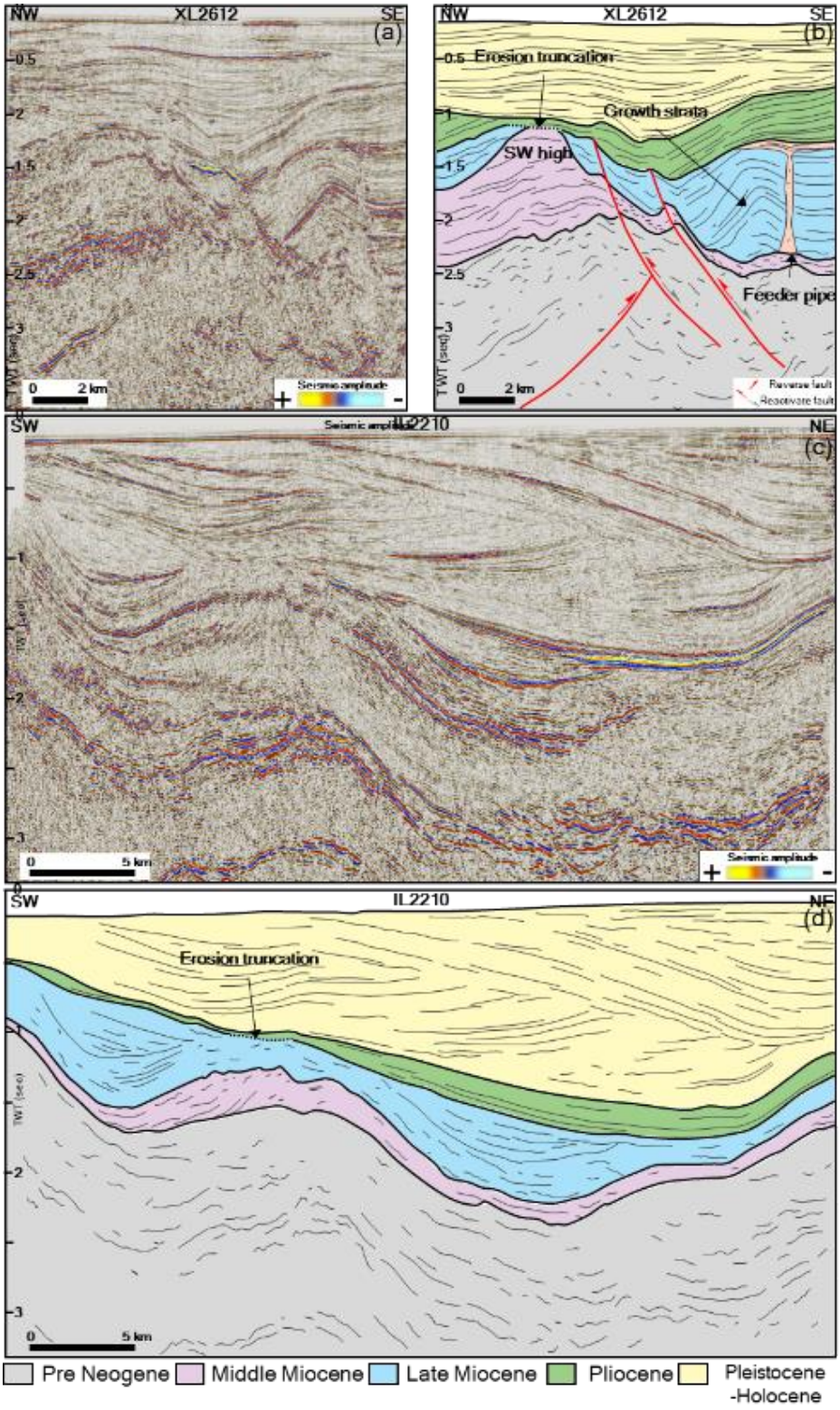


**Figure 5** (a) NW-SE uninterpreted seismic crossline 2612 (b) Corresponding seismic interpretation and internal configuration of crossline 2612 (c) SW-NE uninterpreted seismic inline 2210 (d) Corresponding seismic interpretation and internal configuration of inline 2210. Line locations are shown in Figure 6.

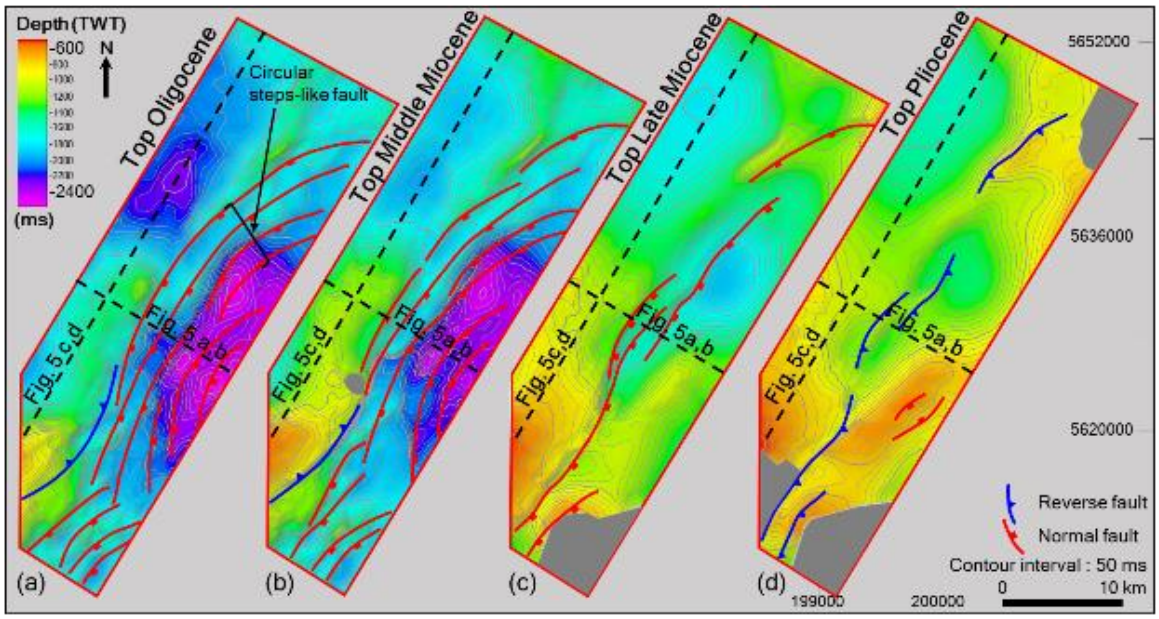


**Figure 6** Time structure maps of (a) Top Oligocene (b) Top Middle Miocene (c) Top Late Miocene (d) Top Pliocene.

## Time structural maps

### Top Oligocene

The Top Oligocene surface has depth ranging from approximately 700 ms to 2590 ms with slight dip to the northeast. There are 3 structural highs within the study area represented by this surface. The faults strike dominantly in NNE-SSW trend (Fig. 6a).

### Top Middle Miocene

The Top Middle Miocene surface has depth ranging from approximately 560 ms to 2590 ms with gentle dip toward the north-northwestern in the northeastern part of the study area. Structural highs and faults strike in the NNE-SSW direction, being similar to the Paleogene sequence. The main depocenter of this map is controlled by south-east dipping circular fault in the eastern part of the study area. (Fig.6b).

### Top Late Miocene

The Top Late Miocene surface has depth ranging from approximately 470 ms to 1890 ms. The structural highs trend dominantly in the NNE-SSW direction. This surface shows abrupt changes in terms of fault segmentation compared to the underlying maps (Fig.6c).

### Top Pliocene

The Top Pliocene surface has depth ranging from approximately 470 ms to 1595 ms. Consistent with the Miocene sequence, structural high trends and faults strike generally in the NNE-SSW direction in the study area (Fig.6d).

## Seismic attributes

In the time slices, the result indicates that the seismic attribute can highlight only fault lineaments in variance attribute. Some of the bright amplitude anomalies in the RMS and sweetness indicate erosional and onlap surfaces. Only a minor area displays the seismic attribute geometry indicative of the deep marine fan lobe.

The seismic surface attributes were also generated along horizon stack. The surface attribute anomalies of above Pliocene (layer: 27; (Fig. 7) show obvious lobe deposit architecture with feeder channel

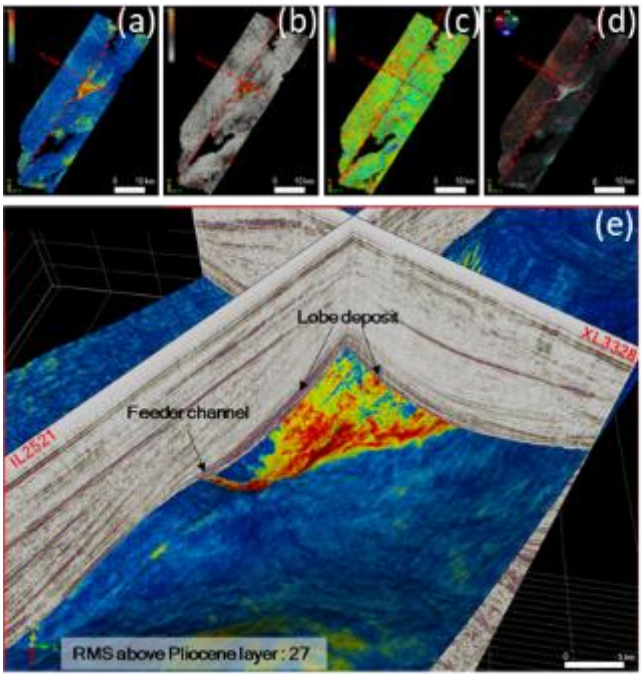


**Figure 7** The result of above Pliocene layer: 27 surface attribute anomalies. (a) RMS (b) Sweetness (c) Instantaneous frequency (d) Spectral decomposition (e) Inline and crossline intersection through observed feature in 3D view.

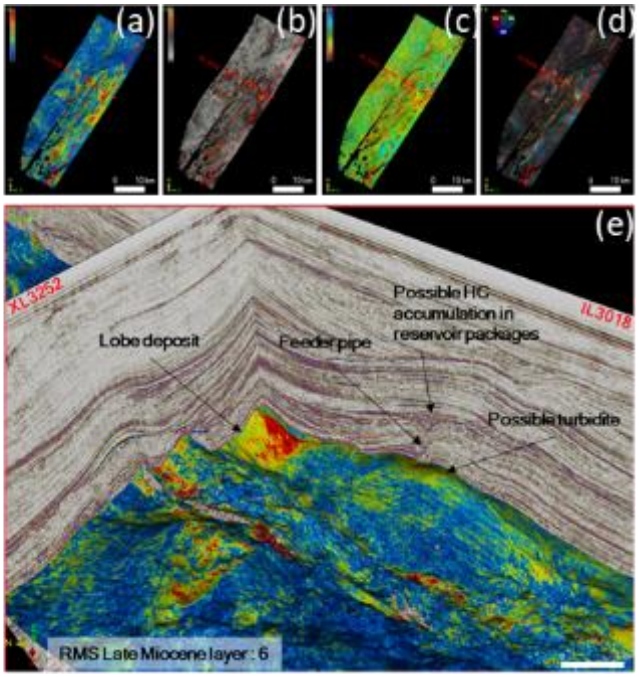


**Figure 8** The result of Late Miocene layer: 6 surface attribute anomalies. (a) RMS (b) Sweetness (c) Instantaneous frequency (d) Spectral decomposition (e) Inline and crossline intersection through observed feature in 3D view.

located in the central part of the study area. Lobe deposit and channel attribute show high RMS amplitude, moderate to high sweetness, low to moderate instantaneous frequency, and visible in the spectral decomposition.

The surface attribute anomalies of Late Miocene (layer: 6; Fig 8) shows lobe architecture with high RMS amplitude, moderate to high sweetness, low to moderate instantaneous frequency, and visible in the spectral decomposition. Possible turbidite was observed on the local high structure in the southeast area and related to the feeder pipe.

For the analysis, this study considers every layer of the surface attribute in order to analyze reservoirs distribution and multiple attributes were also integrated.

## Discussion

From the horizon attribute results, the seismic attribute anomalies above Pliocene layer:27 (Fig. 7) distinctly show lobe and channel shape. The anomalies can indicate transportation of coarse-grained sediments into the deep-water settings by gravity flow. Lobe and channel deposit in the deep-water setting might perform as reservoirs. It is reasonable to assume that the characteristics in each seismic attribute of lobe and channel can be analogous to other possible reservoirs. Consequently, the possible turbidite reservoir might show seismic attribute anomalies, including high RMS amplitude, low to moderate sweetness, and low to moderate instantaneous frequency attributes. Compared to the onlap and truncation surface in the seismic attribute anomalies, the possible turbidite reservoir shows visible but not overly outstanding in the spectral decomposition. The analysis used this analogue concept in order to chase for possible turbidite packages.

According to the geological history of the study area, tectonic movements have the potential to be the cause of the activation of turbidite currents (gravity flow), which are

responsible for transporting coarser grain sediments into deep water environments. The significant shortening in the ECB was caused by thrust faulting during the Miocene. Paleogene and Middle Miocene fault displacement was created by the earliest thrust faulting phase. During that time, the southwest part of the study area developed a structural high. In addition, Early-Middle Miocene sediments were deposited at the same period as the earliest thrust faulting. It appears that the Middle Miocene sequence thins to the northwest area. This information confirms that the tectonic development of the ECB is not a continuous and homogeneous deformation process (Pettinga, 1982; Field et al., 1997; Barnes et al., 2002).

The thrust faulting and reactivation of extensional faults in the Late Miocene might create local highs that contribute as the source of turbidite sediment, whilst subsidence during extensional phase might create low areas. It is possible that the thick turbidite reservoirs ponding behind structural highs and located on the flanks of some structural closures will not always be present on the crests. As a result of structural inversion, some turbidite reservoirs might now be structurally high. Therefore, the possible area for identifying turbidite fairways (Paleo-slope) must be considered as a separate area depending on the fault activities.

Based on horizon interpretation, three structural highs have appeared on the time structural maps since Late Miocene (Fig. 9). Therefore, the study area was divided into three sub-areas to determine the relationship between these three structural highs. Firstly, the Southwestern high (SW high) sub-area was formed by the oldest thrust faulting in the Miocene, which was west dipping fault aligned to the main thrust system as shown in the regional section (Fig. 4).

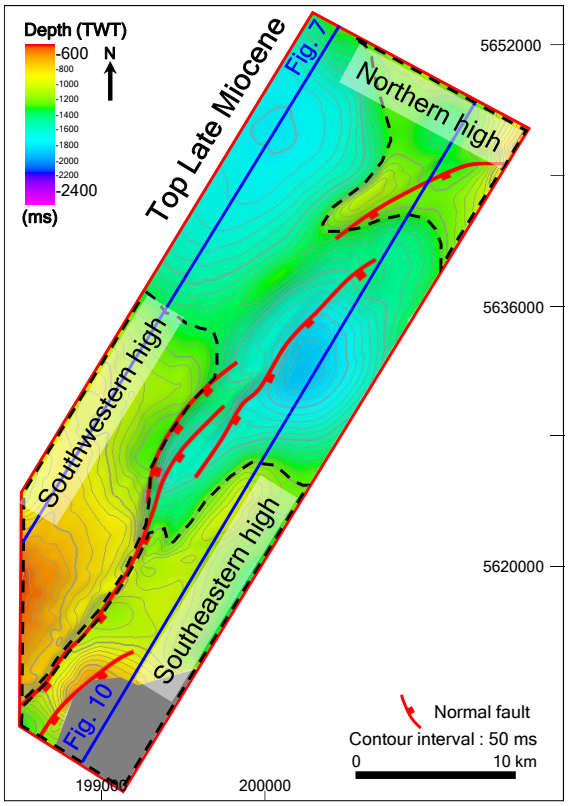


**Figure 9** Time-structural map of the Top Late Miocene displaying sub-area division based on structural high

In addition, significant erosion of Middle – Late Miocene section was observed in this sub-area (Fig.5b). This indicates that the SW high could be the first source of turbidite in the study area.

Therefore, the turbidite pathways might transport the sediment from SW high to low area in the northeast direction. According to the seismic attribute extraction from horizon stacks, the result shows anomalies in Late Miocene packages. The anomalies are distributed from the SW high toward north, which can be inferred as the coarser grain sediment flow to low area. The character of anomalies was displayed in 3D view with high RMS amplitude, high sweetness attribute and ow instantaneous frequency attribute. Moreover, the anomalies appearance shows possible deep marine fan shape in the several seismic attributes and spectral decomposition attribute (Fig. 10).

The second and third sub-areas are the Northern high (N high) and Southeastern high

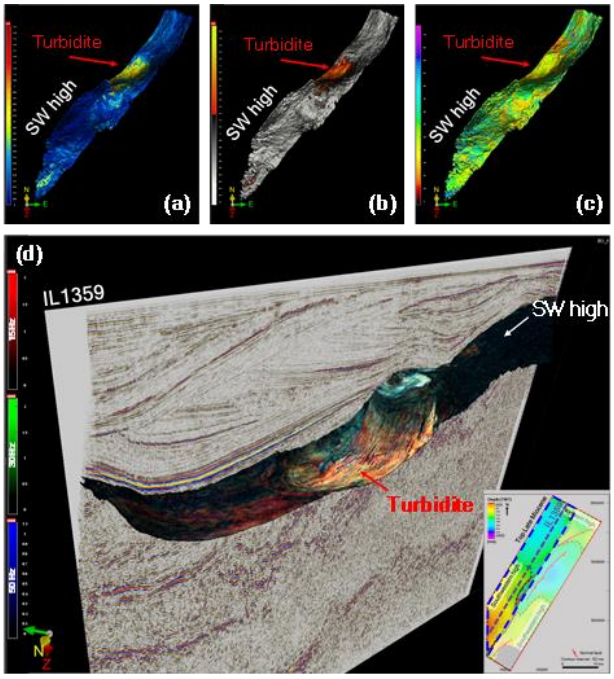


**Figure 10** The example of Miocene horizon attributes displays in 3D view which represent SW high sub-area. (a) RMS attributes (b) Sweetness attributes (c) Instantaneous frequency attributes (d) Spectral decomposition attributes

(SE high) sub-areas, respectively (Fig. 9). During the Latest Miocene to Early Pliocene, back thrust developed from the reactivation of extensional listric faults, forming these two sub-areas structures (Erdi and Huuse, 2018). The stratigraphic thickness at the time of deposition must be considered when interpreting the order of structural high development between these two sub-areas. The horizon flattening could be used to identify the paleogeography of these two sub-areas.

According to the result from horizon flattening, the Miocene packages thin toward the northern high sub-area, which indicates that the N high area was relatively higher than SE high area during the Late Miocene deposition (Fig. 11). Thus, the SE high area was a paleo low, and the turbidite packages would be in the present-day structural high.

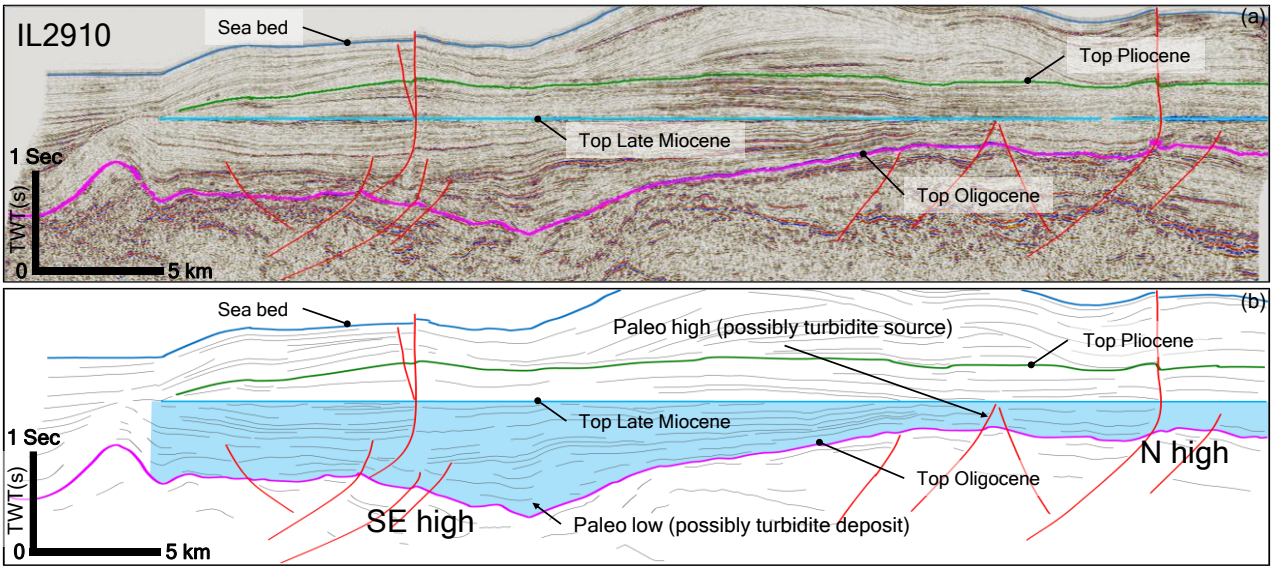


**Figure 11** (a) Seismic profile (inline 2910) flatten on Top late Miocene horizon. (b) Interpretation of (a) showing the Miocene packages thinning toward northern high area which indicates the elevation of N high area was relatively higher than SE high area. Line location is shown in Figures 6 and 8

On the other hand, turbidite packages might be transported southeastward to a lower location of the N high. The example of the seismic attribute anomalies showing the possible turbidite fairways are shown in Figure 12. The characteristics of seismic attribute anomalies are displayed in 3D view with high RMS amplitude, moderate sweetness, and low instantaneous frequency attributes. Moreover, the spectral decomposition attribute anomalies show

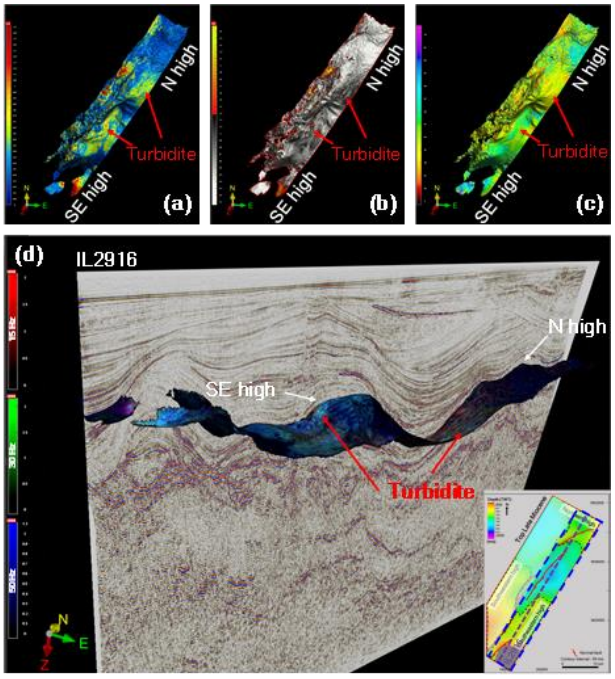


**Figure 12** The example of Miocene horizon attributes displays in 3D view which represent SW high sub-area. (a) RMS attributes (b) Sweetness attributes (c) Instantaneous frequency attributes (d) Spectral decomposition attributes

anomalies spreading which support the hypothesis of possible turbidite fairways.

Hence, the order of the structural highs development in the study area was SW high, followed by N high and SE high, respectively. It can be inferred from local tectonic history and thickness of strata by using horizon flattening technique.

Compared to the area with the same geological setting, Khamis et al. (2018) conducted deformation profile analysis and seismic attribute analysis (both spectral decomposition and simple attributes) in the deep-water fold-thrust belt in the offshore NW Borneo. It was found that the identified sedimentary fairways required structural deformation analysis, which was carried out independently (Khamis et al., 2018).

In the pre-kinematic area, broad unconfined fan geometries cover the yet-to-form structures; during syn-kinematic deformation, sedimentary fairways flow around or through the structures as confined channel fan complexes, before the creation of smaller lobe fans in the synclinal areas. As a comparison, it is noted that the same observations lead to create the simplified model of possible turbidite fairways from sub-horizon attribute anomalies overlaying in Miocene interval (Fig. 13).

The study area is comprised of three main sediment transport pathways. Pathways A and B are located in the low area and they have different sources of turbidite sediment. The SW high supplies sediment to low area in the northeast direction while N high supplies sediment in the southwest direction. Both of the Pathway A and Pathway B are most likely deposited in the piggyback basin of the syncline. The Pathway C is located on the crest structure of the SE high. The direction of sedimentary supply cannot be identified due to deformed condition. Therefore, the possible turbidite packages were in the inner anticlinal fold of SE high.

Pathways C provides the highest potential for hydrocarbon exploration. The huge symmetrical structural closure of the SE high may contain more hydrocarbon than the other two pathways. In addition, the presence of feeder pipe near an anticline structure and the absence of a vertical feeder pipe above the top of the Late Miocene imply the entrapment of hydrocarbon in Late Miocene interval (Fig. 5b and 8e). Therefore, pathways C is the most promising compared to the other pathways.

## Conclusion

The order of structural evolution is the most essential consideration when investigating turbidite packages in this study area due to the non-continuous and heterogeneous deformation process in each area. The order of three

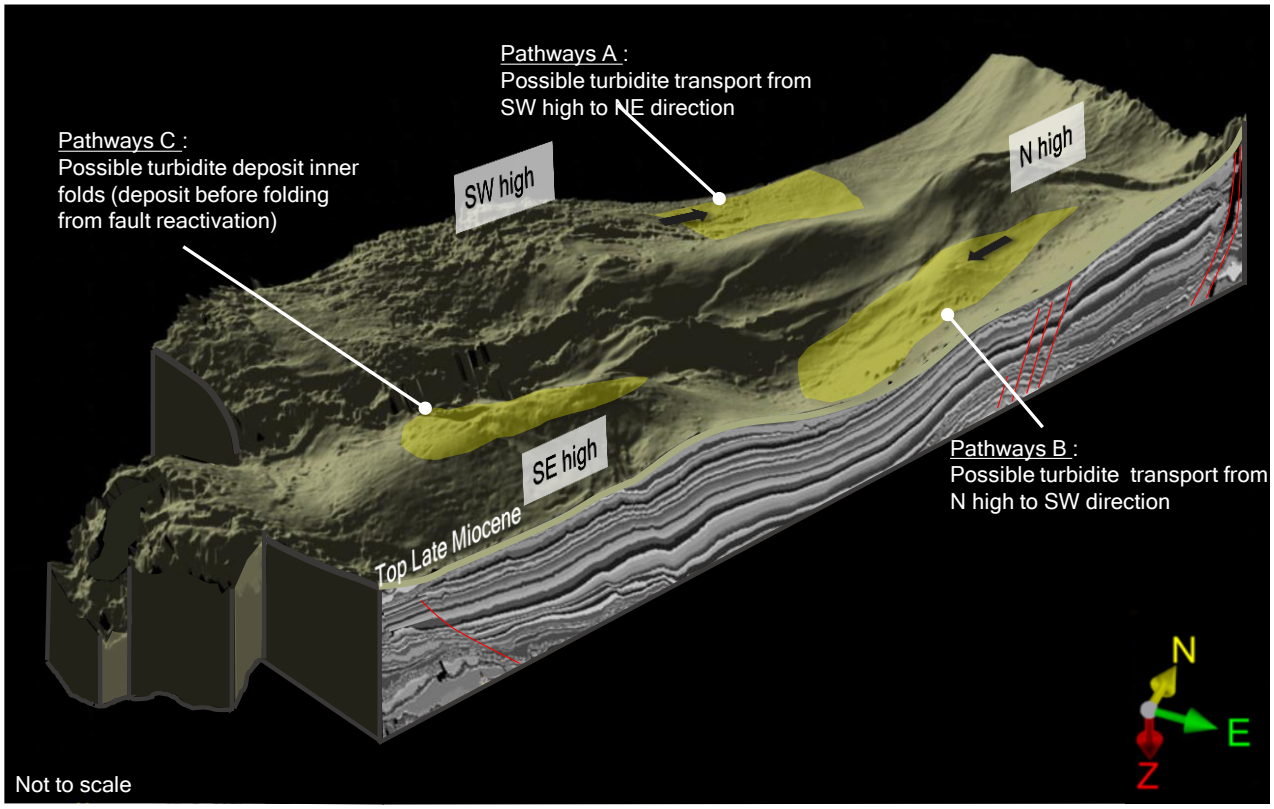


**Figure 13** Simplify model of possible turbidite fairways (yellow areas) on the Late Miocene time structural map.

structural high development was SW high followed by N high and SE high, respectively. It can be inferred from the thickness of strata by using horizon flattening technique.

In the Miocene interval, the turbidite system pathways can be separated into three pathways. The first zone is the path where sediments are transferred from the SW high to the NE direction. The second zone is the pathway from N high. The sediments are transported to the basin toward SW direction in the central part of the study area. The third zone is located on the SE high. The SE high was a paleo low, hence the turbidite package was transported to this part of study area, which is the present-day peak of SE high area.

The prospective location of turbidite fairways in the study area that is beneficial for hydrocarbon exploration is located in the southeast high, which has a large anticline structure and has very thick packages of Neogene sediment. In addition, the seismic data identified fluid-related features that imply an active petroleum system in this sub-area.

## Acknowledgements

Sincere gratitude is extended to PTTEP for providing the first author with a scholarship to study a Master of Science in Petroleum Geoscience at Department of Geology, Chulalongkorn University. New Zealand Petroleum and Minerals is acknowledged for the data used for this project. In addition, Schlumberger is acknowledged for providing the Petrel software. Eliis is acknowledged for academic use of the PaleoScan™ software.

## References

Barnes, P., Nicol, A., and Harrison, T. 2002. Late Cenozoic evolution and earthquake potential of an active listric thrust complex above the Hikurangi subduction zone, New Zealand. Geological Society of

America Bulletin, v. 114, no. 11, p.1379–1405.

Barnes, P., Lamarche, G., Bialas, J., Henrys, S., Pecher, I., Netzeband, G.L., Greinert, J., Mountjoy, J., Pedley, K., Crutchley, G. 2010. Tectonic and geological framework for gas hydrates and cold seeps on the Hikurangi subduction margin, New Zealand. Marine Geology, Volume 272, Issues 1–4, p26–48.

Bland, K., Kamp, P.J.J, Nelson, C.S. 2004. Stratigraphy and development of the Late Miocene-Early Pleistocene Hawke's Bay forearc basin. New Zealand Petroleum Conference Proceedings.

Brown, I., 2002, Kehe, Koheru and Hiwihiwi prospects. Ministry of Economic Development New Zealand. Open-file Petroleum Report 2939 Ministry of Economic Development, Wellington, New Zealand

Burgreen-Chan, B., Meisling, K. and Graham, S. 2015. Basin and petroleum system modelling of the East Coast Basin, New Zealand: a test of overpressure scenarios in a convergent margin. Basin Res 28(4), 536–567

Davies, E., Frederick, J., Leask, W., Williams, T., 2000. East Coast drilling results, 2000 New Zealand Petroleum Conference. Ministry of Commerce, Wellington, New Zealand, p. 11.

Dobbie, W.A., Carter, M.J., 1990. Te Hoe-1 well completion report PPL 38316. Ministry of Economic Development New Zealand petroleum report PR 1835.

Erdi A. & Huuse M., 2018. Tectonic Evolution and Hydrocarbon Prospectivity of East Coast Basin, Offshore Hawke Bay, New Zealand. OTC-28212-MS

Field, B., 2005. Cyclicity in turbidites of the Miocene Whakataki Formation, Castlepoint, North Island, and implications for hydrocarbon reservoir modelling. New Zealand Journal of Geology and Geophysics 48, 135-146.

Field, B.D., Uruski, C.I. 1997. Cretaceous-Cenozoic geology and petroleum systems of the East Coast region, New Zealand. Institute of Geological & Nuclear Sciences, Lower Hutt, New Zealand. Institute of Geological & Nuclear Sciences monograph 19. 301 p.

Francis, D.A., 1994. Reservoir formations in western and northern Hawke’s Bay, East Coast Basin, New Zealand. PPP38324, PPL38316. Petrocorp Exploration NZ Ltd. Ministry of Economic Development New Zealand Unpublished Petroleum Report PR2160.

Francis, D.A., 1995. Reservoir potential of the East Coast oil and gas province. Petroleum exploration in New Zealand news 45, 11-19.

Francis, D.A., 1998. The real oil and a bit of gas on East Coast reservoirs, 1998 New Zealand Petroleum Conference, pp. 207-221.

Francis, D., Bennett, D., Courteney, S., 2004. Advances in understanding of onshore East Coast Basin structure, stratigraphic thickness and hydrocarbon generation, 2004 New Zealand Petroleum Conference.

Griffin, A.G., Bland, K.J., Field, B.D., Strogen, D.P., Crutchley, G.J., Lawrence, M.J.F., Kellett, R., 2015. Reservoir characterisation of the East Coast and Pegasus Basins, eastern North Island, New Zealand, AAPG/SEG International Conference & Exhibition 2015. AAPG

Search and Discovery, Melbourne, Australia, 13–16 September 2015.

Khamis, M. A., Jong, J. & Barker, S.M., 2018. Deformation Profile Analysis of a Deepwater Toe-Thrust Structural Trend - Implications on Structural Kinematics and Sedimentary Patterns. Bulletin of the Geological Society of Malaysia, Volume 65, June 2018, pp. 1 – 12.Mazengarb, C., Speden, I.G., 2000. Geology of the Raukumara Area: Institute of Geological and Nuclear Sciences 1: 250,000 geological map 6. Institute of Geological and Nuclear Sciences Limited, Lower Hutt, New Zealand.

Mortimer, N. 2004. New Zealand's Geological Foundations. Gondwana Res., 7(1), 261–272.New Zealand Petroleum & Minerals. 2014. New Zealand Petroleum Basins 2014/2015 Revised Edition. Ministry of Business, Innovation and Employment. www.nzpam.govt.nz

Paquet, F., Proust, J-N., Barnes, P.M., Pettinga, J.R. 2011.Controls on active forearc basin stratigraphy and sediment fluxes: The Pleistocene of Hawke Bay, New Zealand. GSA Bulletin; 123 (5-6): 1074–1096.

Pettinga, J.R. 1982. Upper Cenozoic structural history, coastal Southern Hawke's Bay, New Zealand. N. Z. J. Geol. Geophys., 25, 149–191

Strogen, D.P., Field, B.D., Browne, G.H., 2010. Petrography of sandstones from the Miocene Tunanui Formation, Hawke's Bay, New Zealand. GNS Science Report 2010/32. 49 p., Lower Hutt.

Totake, Y., Butler, R.W.H., Bond, C.E. &Aziz, A., 2017. Analysing Structural Variations Along Strike in a Deepwater Thrust Belt. Journal of Structural Geology.